Electronic and optical properties of LiBC

A. V. Pronin,[1,2,*] K. Pucher,[1] P. Lunkenheimer,[1] A. Krimmel,[1] and A. Loidl[1]
[1]*Experimentalphysik V, Elektronische Korrelationen und Magnetismus, Institut für Physik, Universität Augsburg, 86135 Augsburg, Germany*
[2]*Institute of General Physics, Russian Academy of Sciences, 119991 Moscow, Russia*
(Received 12 July 2002; published 10 April 2003)

LiBC, a semiconducting ternary borocarbide constituted of the lightest elements only, has been synthesized and characterized by x-ray powder diffraction, dielectric spectroscopy, and conductivity measurements. Utilizing an infrared microscope the phonon spectrum has been investigated in a quasi-single-crystalline sample. The in-plane B-C stretching mode has been detected at 150 meV, noticeably higher than in AlB_2, a nonsuperconducting isostructural analog of MgB_2. It is this stretching mode, which reveals a strong electron-phonon coupling in MgB_2, driving it into a superconducting state below 40 K, and is believed to mediate high-temperature superconductivity predicted in hole-doped LiBC [H. Rosner, A. Kitaigorodsky, and W. E. Pickett, Phys. Rev. Lett. **88**, 127001 (2002)].

DOI: 10.1103/PhysRevB.67.132502 PACS number(s): 74.25.Kc, 63.20.−e, 74.25.Gz, 77.22.Ch

The discovery of phonon-mediated superconductivity in MgB_2 with a superconducting transition temperature of $T_c \sim 40$ K (Ref. 1) has triggered enormous interest in similar layered compounds. MgB_2 consists of graphitelike boron layers with the Mg ions intercalated in between. The B-B bonding σ bands reveal a two-dimensional character and are strongly coupled to the in-plane stretching mode, consistent with a phonon-mediated BCS type pairing mechanism.[2] In Raman and neutron scattering experiments,[3,4] an extremely strong renormalization of this stretching mode has been unambiguously demonstrated. The authors found that the in-plane boron vibration in MgB_2 is shifted to 70 meV, while in the isostructural but nonsuperconducting AlB_2 it is located at 123 meV. From the averaged phonon density and the electron-phonon coupling, the superconducting transition temperatures can be estimated and the theoretical estimates using a strong electron-phonon coupling deduced superconducting transition temperatures of the correct magnitude.[3,5] Similar layered compounds have been theoretically investigated[6–8] and a superconducting transition temperature of $T_c \sim 120$ K has been predicted for hole-doped LiBC by Rosner *et al.*[7]

Since the mid 1980's, LiBC was a subject of only a few experimental studies.[9,10] It reveals the same structure as MgB_2, but with the planar hexagonal boron layers replaced by B-C layers, with the B and C atoms alternating both within the layer and along the c direction. LiBC has $P6_3/mmc$ symmetry with $a = 0.275$ nm and $c = 0.7058$ nm.[10] The stoichiometric compound is insulating. From band structure calculations, a gap of at least 1 eV has been deduced for the pure compound and it has been shown that on hole doping, induced by Li deficiency, the σ bands significantly contribute to the Fermi level and are strongly coupled to the B-C stretching mode.[7]

In this work, we synthesized powder and single crystalline LiBC, characterized the samples by x-ray powder diffraction, determined the dielectric constant and the conductivity as function of temperature, and measured the optical properties in the far-infrared and mid-infrared range. Besides the interesting question of the phonon renormalization in hole-doped compounds, which should be the subject of further studies, it certainly also is highly interesting to investigate a ternary compound synthesized from the lightest elements only.

LiBC was synthesized from the elements at 770 K with subsequent annealing at 1770 K in sealed niobium ampoules with open molybdenum crucibles inside. The molybdenum crucibles, 5 mm diameter and approximately 50 mm length, have been filled in an argon box with commercially available lithium, boron, and carbon with a lithium excess of 300% compared to the stoichiometric ratio. This excess is necessary to provide a high lithium vapor pressure in the ampoule. The carbon and boron powders were preliminarily annealed in vacuum. The Mo crucibles have been placed in Nb ampoules, the latter sealed by argon welding. It is known, that molybdenum does not react with any of the components, while it cannot hold high pressures at high temperatures. Due to this fact an additional niobium ampoule is necessary. The use of a Nb ampoule only is impossible since niobium reacts with boron. This sample preparation technique has been developed in the groups of Nesper (Zürich) and von Schnering (Stuttgart), and is described in detail in Refs. 9,10. The ampoules have been heated up to 770 K with a rate 100 K/h, held at 770 K for one hour, then heated up to 1770 K with 200 K/h, held one more hour at this temperature, and finally, cooled down with a rate of approximately 150 K/h. Faster cooling seems to support the growth of crystals of larger size. After removing the extra lithium, the product consists of mainly yellow golden powder. Some crystals can be quite large reaching the size of $0.5 \times 0.5 \times 0.01$ mm^3.

One of these platelets is demonstrated in Fig. 1. The hexagonal morphology is clearly indicated by the terraced ideal hexagon shown in the inset 2 in Fig. 1. We believe our samples have highly preferred crystallographic orientation with B-C planes parallel to the largest faces of the sample. Since the infrared reflectivity measurements from these large faces, described below, show some amount of the out-of-B-C-plane response, we consider the samples as aligned polycrystals or quasi single crystals, rather than single crystals.

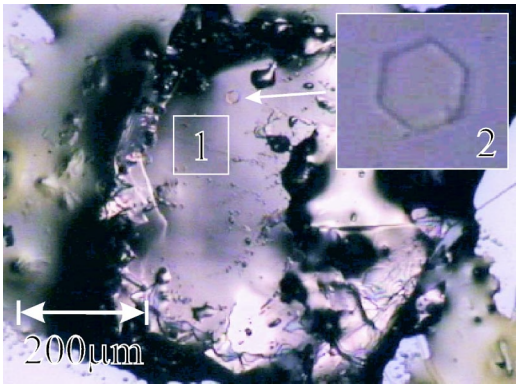

FIG. 1. (Color online) Photograph of a LiBC crystalline sample. The area (1) shows an example of the sample region investigated in the infrared experiments. The inset (2) shows a magnification of a little terrace on the sample surface with a perfect hexagonal shape.

The x-ray powder diffraction measurements have been performed at room temperature using a commercial diffractometer with a position sensitive detector utilizing Cu-K_α radiation with $\lambda = 0.1541$ nm. The data have been analyzed by standard Rietfeld refinement. The diffraction pattern has shown the correct symmetry ($P6_3/mmc$) with no indications of spurious phases. The lattice constants, $a = 0.2751(1)$ nm and $c = 0.7055(1)$ nm, were found in good agreement with published results.[10]

The dc resistivity of a quasi single crystal was measured using a standard four-point technique in the range 3 K$< T <$300 K. Using a coplanar contact geometry the electrical field was directed parallel to the largest sample surfaces (B-C layers). The contacts were prepared by silver paint. Due to the ill-defined geometry of the rather small sample, the absolute values of the resistivity should be taken as a rough estimate only. As is shown in Fig. 2, the temperature dependence of the resistivity exhibits semiconducting characteristics, however, only with a rather small overall change of about a factor of 3 in the investigated temperature range. It does not follow a thermally activated behavior, $\rho \propto \exp(E/T)$. Also the prediction of the variable range hopping model $\rho \propto \exp(B/T^{1/4})$, which often can be applied for hopping conduction of localized charge carriers,[11] does not work for LiBC. Instead, in a rather broad temperature range the resistivity can be phenomenologically described by a power law $\rho \propto T^{-n}$, as demonstrated in the double-logarithmic representation in the inset of Fig. 2 revealing an exponent $n \approx 0.23$. However, we are not aware of any theoretical model that could explain such a power-law behavior.

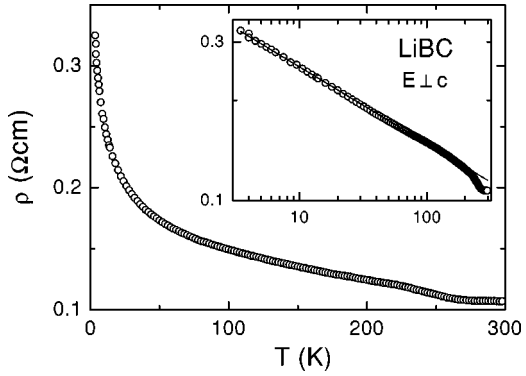

FIG. 2. Temperature dependence of the dc resistivity of LiBC, measured with the field parallel to the largest sample faces (mostly parallel to the B-C planes) using four-point contact configuration. The inset shows the same data in a double-logarithmic representation, the line demonstrating an approximate T^{-n} power-law behavior with $n \approx 0.23$.

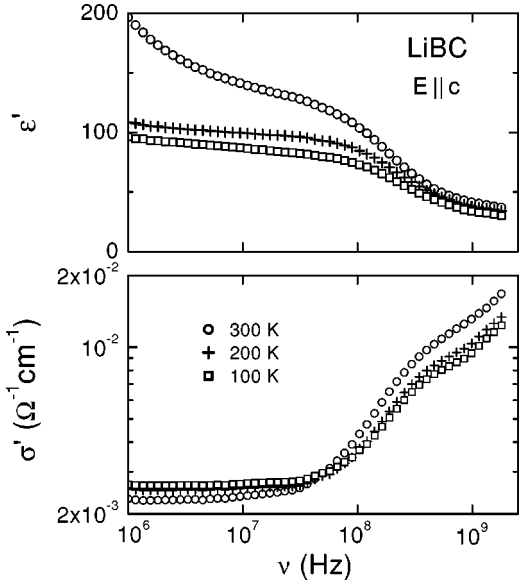

FIG. 3. Frequency dependence of the real parts of the dielectric constant ε' and ac conductivity σ' of LiBC for three temperatures. The measurements were performed using a two-point contact configuration with the electric field directed perpendicular to the largest sample surfaces (mostly perpendicular to the B-C planes).

In addition, the dielectric properties of the platelet-shaped samples were measured in sandwich geometry, i.e., with the field directed perpendicular to the largest sample faces (mostly perpendicular to the B-C layers). The measurements were performed for frequencies $10^6 \leqslant \nu \leqslant 2 \times 10^9$ Hz employing a reflectometric technique, described in detail in Ref. 12. Fig. 3 shows the frequency dependence of the dielectric constant ε' and the conductivity σ' for three temperatures. $\varepsilon'(\nu)$ exhibits a step-like decrease with the point of inflection close to 300 MHz, $\sigma'(\nu)$ an increase with a shoulder near the same frequency. Such a behavior could be indicative of a dipolar relaxation process, but as the existence of dipolar entities in LiBC is unlikely, a nonintrinsic origin of the observed relaxationlike features seems to be more reasonable. Thus we ascribe this behavior to Maxwell-Wagner type contributions of the interface between sample and contacts. As demonstrated in detail in Ref. 13, the intrinsic response is revealed at high frequencies only, when the contact resistance is bridged by the contact capacitance acting like a short at high frequencies. From Fig. 3, close to 1 GHz we read off a value of $\varepsilon' \approx 35$, which smoothly saturates towards higher frequencies and is nearly temperature independent. From the frequency dependence of $\sigma'(\nu)$ in the intrinsic region at $\nu >$300 MHz a plateau, followed by a further increase, can be

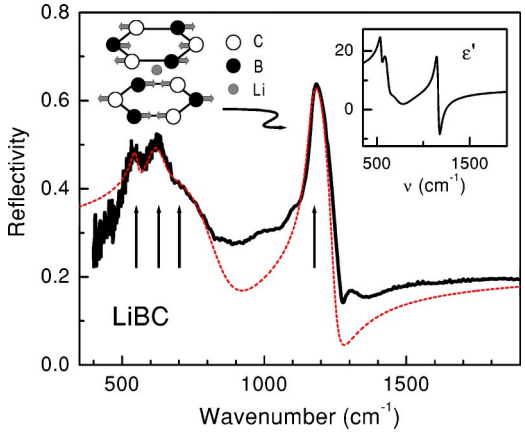

FIG. 4. (Color online) Reflectivity of a LiBC crystal in the far- and mid-infrared range. The vertical arrows mark the phonon positions. The dashed line is a fit of the experimental spectra with four Lorentz oscillators. The inset shows the dielectric permittivity calculated from the fit of the reflectivity data. The displacement pattern of the B-C stretching infrared-active mode is shown in the upper left corner.

suspected, which would be indicative of hopping conduction of localized charge carriers.[14] Measurements at even higher frequencies are necessary to corroborate this conjecture. Within this picture, the plateau represents the intrinsic dc conductivity, which can be read of as $\sigma_{dc} \approx 10^{-2}\ \Omega^{-1}\mathrm{cm}^{-1}$, showing a weak temperature dependence only.

Thus, the dc resistivity perpendicular to the B-C planes seems to be more than two orders of magnitude higher than the measured dc resistivity parallel to the planes (cf. Fig. 2) indicating a strong anisotropy of the electrical transport properties. Since the measurements are influenced by the imperfect shape of the crystalline platelets, leading to some mixing of the in-plane and out-of-plane responses, the resistivity and the dielectric constant data should be considered as rough, but reliable estimates. Measurements on perfect single crystals with regular shape may show even higher values of the anisotropy.

The measurements of the optical reflectivity were carried out using the infrared microscope Bruker IRscope II, which was connected to a Fourier-transform infrared spectrometer Bruker IFS 66v/S. The measurements were made on flat surfaces of as-grown crystals at frequencies from 400 to 2000 cm^{-1}. In order to eliminate multiple reflections from the opposite sides of the plane-parallel samples, the samples were tilted by a small angle (no more than 10°) to the normal incidence. Using the infrared microscope, we were able to focus on a small fraction of the LiBC platelets with the best flatness compared to surrounding areas. An example of such an investigated area is shown in Fig. 1.

The reflectivity as obtained from the infrared measurements is shown in Fig. 4. We observe three well-defined peaks in the spectrum at 540, 620, and 1180 cm^{-1}, and assign them to the infrared active phonons. A large shoulder at 700 cm^{-1} most likely represents the forth optical phonon. It should be noted that the quasiperiodic variation of R, visible in the spectra, is the residual influence of the multiple reflections inside the sample, which could not be completely removed by tilting the sample. This interference pattern is most clearly seen at 1300 cm^{-1}, and also between 800 and 1100 cm^{-1}. A spectra measured closer to the normal incidence reveal much more pronounced fringes. These oscillations make a quantitative analysis quite difficult, and the fit with four Lorenzians, shown in Fig. 4 by a dashed line, is not ideal. The inset in Fig. 4 shows the dielectric permittivity ε' as calculated from the fit of the reflectivity spectrum. Since the description of the reflectivity is not perfect, the data for ε' are subject to large errors. However, we would like to stress that $\varepsilon' \approx 15$ in the terahertz regime is not too far from $\varepsilon' \approx 35$ as measured at 1 GHz, having in mind that the intrinsic value still is not quite reached at this frequency. The remaining difference most likely is due to a relative large uncertainty in the determination of the crystal thickness, which affects the absolute values of ε' in the dielectric measurements.

The group analysis for LiBC ($P6_3/mmc$, D_{6h}^4) yields the following modes at the Γ point: $3A_{2u}+2B_{1g}+B_{2u}+3E_{1u}+E_{2u}+2E_{2g}$, four of which are optical infrared-active modes ($2A_{2u}$ and $2E_{1u}$). The four modes observed in our measurements most likely represent these infrared-active phonons. Although the reflectance was measured from quite plane sample surfaces, which are supposed to be mostly parallel to the B-C planes, we believe that a significant amount of the out-of-plane response is also present in our measurements. The tilted geometry of the reflectivity measurements probably further increases the out-of-plane contribution.

If one compares the observed absolute values of the phonon frequencies in LiBC with those observed and calculated for aluminum diboride,[3,4] one immediately finds a close similarity. In both compounds there is a very high-frequency phonon, which is a Raman-active E_{2g} mode in AlB_2 at $\sim$980 cm^{-1} (123 meV) and the mode at 1180 cm^{-1} ($\sim$150 meV) in our measurements of LiBC. We ascribe this mode to the E_{1u} infrared-active phonon. Due to the doubling of the unit cell in LiBC compared to AlB_2, the stretching Raman active E_{2g} mode of the B-B hexagons transforms into two modes in LiBC, E_{2g} and E_{1u}. The latter is infrared active, its displacement pattern is shown in Fig. 4. The E_{2g} mode in AlB_2 has been shown to soften considerably on doping this compound with Mg, which is accompanied by the onset of superconductivity in $Mg_{1-x}Al_xB_2$ (Ref. 4). This softening is believed to result from the electron-phonon renormalization driving the superconductivity in magnesium diboride.

The three other infrared modes in LiBC have lower frequencies and are situated quite close to each other, resembling again the situation in AlB_2, where two infrared-active modes are supposed to exist in the range 300–500 cm^{-1} (Refs. 3,4). The moderate upward shift in the frequencies of the observed modes in LiBC compared to the modes in AlB_2 is due to the fact that LiBC consists of lighter elements.

The modes observed in our infrared study are in agreement with very recent Raman results[15] and have already been used to fine-tune lattice dynamic calculations of LiBC.[16] According to these calculations, the highest frequency phonon at $\sim$1200 cm^{-1} indeed corresponds to the B-C bond stretch-

ing mode with E_{1u} symmetry. A comparison of the lower frequency modes with theoretical predictions, requires calculations of the dynamical effective charges Z^*, which have not been done yet.

Concluding this section, we mention that we have extended the infrared measurements up to approximately 1 eV and found no indication of the onset of an interband transition, demonstrating that the band gap is substantially larger than 1 eV. In the local density approximation calculations of Rosner *et al.*, valence and conduction bands are separated by 1 eV. Band gaps between 2.5 and 4.2 eV have been calculated by Wörle *et al.*[10]

In conclusion, we have synthesized powder and crystalline samples of ternary borocarbide LiBC and characterized them by x-ray diffraction. The dc resistivity and ac dielectric measurements, performed on samples with highly preferred crystallographic orientation (quasi single crystals), demonstrate semiconducting temperature characteristics and manifest a strong anisotropy in LiBC ($\rho_{\parallel c}/\rho_{\perp c} \geqslant 100$). Infrared spectroscopy utilizing an infrared microscope reveals four infrared-active phonon modes, consistent with point-group symmetry considerations. The high-frequency mode at 150 meV can be ascribed to the B-C stretching mode. It is this phonon mode that is expected to drive phonon-mediated superconductivity in hole-doped LiBC at temperatures substantially higher than in MgB_2 (Ref. 7). The next step is to follow the softening of this in-plane mode as a function of Li deficiency.

Note added in proof. The Born effective charges and the infrared response of LiBC have been recently calculated by Lee and Pickett.[17]

We would like to thank U. Killer, F. Mayr, M. Müller, A. Pimenova, and D. Vieweg for the experimental support. A.V.P. is also grateful to J. Hlinka and J. Petzelt for valuable consultations. This work was partly supported by the DFG via the Sonderforschungsbereich 484 (Augsburg) and by the BMBF via the Contract No. EKM/13N6917/0.

*Electronic address: artem.pronin@physik.uni-augsburg.de

[1] J. Nagamatsu, N. Nakagawa, T. Muranaka, Y. Zenitani, and J. Akimitsu, Nature (London) **410**, 63 (2001).

[2] See, for example, J.M. An and W.E. Pickett, Phys. Rev. Lett. **86**, 4366 (2001); J. Kortus, I.I. Mazin, K.D. Belashchenko, V.P. Antropov, and L.L. Boyer, Phys. Rev. Lett. **86**, 4656 (2001); G. Satta, G. Profeta, F. Bernardini, A. Continenza, and S. Massidda, Phys. Rev. B **64**, 104507 (2001).

[3] K.-P. Bohnen, R. Heid, and B. Renker, Phys. Rev. Lett. **86**, 5771 (2001).

[4] B. Renker, K.B. Bohnen, R. Heid, D. Ernst, H. Schober, M. Koza, P. Adelmann, P. Schweiss, and T. Wolf, Phys. Rev. Lett. **88**, 067001 (2002).

[5] Y. Kong, O.V. Dolgov, O. Jepsen, and O.K. Andersen, Phys. Rev. B **64**, 020501 (2001).

[6] P. Ravindran, P. Vajeeston, R. Vidya, A. Kjekshus, and H. Fjellvåg, Phys. Rev. B **64**, 224509 (2001).

[7] H. Rosner, A. Kitaigorodsky, and W.E. Pickett, Phys. Rev. Lett. **88**, 127001 (2002).

[8] P.P. Singh, cond-mat/0201126 (unpublished).

[9] G. Mair, Ph.D. thesis, University of Stuttgart, 1984; M. Schwarz, Ph.D. thesis, University of Stuttgart, 1987.

[10] M. Wörle, R. Nesper, G. Mair, M. Schwarz, and H.G. von Schnering, Z. Anorg. Allg. Chem. **621**, 1153 (1995).

[11] N.F. Mott and E.A. Davis, *Electronic Processes in Non-Crystalline Materials* (Clarendon Press, Oxford, 1979).

[12] R. Böhmer, M. Maglione, P. Lunkenheimer, and A. Loidl, J. Appl. Phys. **65**, 901 (1989); U. Schneider, P. Lunkenheimer, A. Pimenov, R. Brand, and A. Loidl, Ferroelectrics **249**, 89 (2001).

[13] P. Lunkenheimer, V. Bobnar, A.V. Pronin, A.I. Ritus, A.A. Volkov, and A. Loidl, Phys. Rev. B **66**, 052105 (2002).

[14] A.K. Jonscher, *Dielectric Relaxations in Solids* (Chelsea Dielectrics, London, 1983).

[15] J. Hlinka, I. Gregora, J. Pokorny, A.V. Pronin, and A. Loidl, Phys. Rev. B **67**, 020504 (2003).

[16] J.M. An, H. Rosner, S.Y. Savrasov, and W.E. Pickett, Physica B **328**, 1 (2003).

[17] K.-W. Lee and W.E. Pickett, cond-mat/0302488 (unpublished).